
Interlaminar fracture studies in Portugal: past, present and future

A.B. de Morais^{1*}, C.C. Rebelo², P.M.S.T. de Castro³, A.T. Marques³ and P. Davies⁴

¹Department of Mechanical Engineering, University of Aveiro, Campus Santiago, 3810-193 Aveiro, Portugal

²Department of Mechanical Engineering, Polytechnic Institute of Coimbra, Institute of Engineering, Rua Pedro Nunes – Quinta da Nora, 3030-199 Coimbra, Portugal

³Faculty of Engineering, Department of Mechanical Engineering and Industrial Management, University of Porto, Rua Dr. Roberto Frias, 4200-465 Porto, Portugal

⁴Materials and Structures group, IFREMER, Centre de Brest BP70, 29280 Plouzané, France

*: Corresponding author : : A. B. de Morais. E-mail: abm@mec.ua.pt

Abstract: This paper reviews the state-of-the-art in interlaminar fracture testing of composite materials, with particular emphasis on the work performed in Portugal over the last 15 years. Early work, carried out within the ESIS Polymer and Composite Technical Committee, was concerned with improving test methods on unidirectional [0°]_n specimens. The focus was on the mode I double cantilever beam (DCB) test and on mode II end-notched flexure (ENF) and end loaded split (ELS) tests. In spite of some remaining controversy on mode II testing, the main issue nowadays is fracture toughness measurement on multidirectional specimens. Remaining difficulties are discussed in the light of the most recent work. Guidelines for ongoing and future research are also presented.

Keywords: double-cantilever-beam-DCB; end-notched-flexure-ENF; interlaminar-fracture; multidirectional-laminates; unidirectional-laminates

INTERLAMINAR FRACTURE STUDIES IN PORTUGAL: PAST, PRESENT AND FUTURE

A. B. de Morais^{1,*}, C. C. Rebelo², P. T. de Castro³, A. T. Marques³, P. Davies⁴

¹University of Aveiro, Department of Mechanical Engineering, Campus Santiago, 3810-193 Aveiro, Portugal.

²Politechnic Institute of Coimbra, Institute of Engineering, Department of Mechanical Engineering, Rua Pedro Nunes - Quinta da Nora, 3030-199 Coimbra, Portugal.

³University of Porto, Faculty of Engineering, Department of Mechanical Engineering and Industrial Management, Rua Dr. Roberto Frias, 4200-465 Porto, Portugal.

⁴Materials and Structures group, IFREMER, Centre de Brest BP70, 29280 Plouzané, France.

* Corresponding author, Tel. 234 370830; Fax. 234 370953; E-mail: abm@mec.ua.pt

ABSTRACT

This paper reviews the state-of-the-art in interlaminar fracture testing of composite materials, with particular emphasis on the work performed in Portugal over the last 15 years. Early work, carried out within the ESIS Polymer and Composite Technical Committee, was concerned with improving test methods on unidirectional $[0^\circ]_n$ specimens. The focus was on the mode I Double Cantilever Beam (DCB) test and on mode II End Notched Flexure (ENF) and End Loaded Split (ELS) tests. In spite of some remaining controversy on mode II testing, the main issue is nowadays fracture toughness measurement on multidirectional specimens. Remaining difficulties are discussed in the light of the most recent work. Guidelines for ongoing and future research are also presented.

Keywords: Interlaminar fracture; Double Cantilever Beam (DCB); End Notched Flexure (ENF); unidirectional laminates; multidirectional laminates.

1. INTRODUCTION

Polymer matrix composites have become highly relevant structural materials, owing to their high stiffness and strength combined with low weight. However, the usual laminated nature and the relatively low matrix strength make them particularly susceptible to delamination. For example, low velocity impact can generate relatively large delaminations, which are highly detrimental to compressive strength because of localised buckling phenomena. The characterisation of delamination resistance is thus highly relevant for design of composite

parts. The main delamination resistance parameters of composites are the critical strain energy release rates, G_c , measured in interlaminar fracture tests.

This paper addresses the state-of-the-art in mode I and mode II testing, which is illustrated with results obtained by the authors. Finally, current and future research guidelines are described.

2. UNIDIRECTIONAL LAMINATES

2.1. Mode I

The mode I Double Cantilever Beam (DCB) test (figure 1) is nowadays standardised for G_{Ic} measurements on unidirectional (UD) $[0^\circ]_n$ specimens^{1,2}. In these tests, the load P and the displacement δ recorded for specified crack positions a are usually processed with the Corrected Beam Theory (CBT)

$$G_{Ic} = \frac{3P\delta}{2b(a+|\Delta|)} \frac{F}{N}, \quad (1)$$

where b is the specimen width, typically 20 mm, Δ is a correction for crack tip rotation and deflection, determined from a linear regression analysis of $(\delta/PN)^{1/3}$ versus crack length (a) data, F is a correction factor for large displacements and N is a correction factor for the stiffening caused by the metal blocks^{1,2}.

Most composites present an R -curve, which can be quite pronounced for thermoplastic matrix composites³⁻⁵. Figure 2 depicts results obtained from C/PEEK⁵ and C/epoxy specimens⁶. R -curves are generally associated with fibre bridging between the arms of the specimen, a phenomenon that is specific to the DCB specimen. Therefore, it is quite important to obtain accurate initiation values, $G_{Ic,i}$, and this is an issue that has not yet been completely solved.

The first question is whether $G_{Ic,i}$ should be measured from the film generated starter crack or from a mode I precrack. It was shown that $G_{Ic,i}$ becomes independent of film thickness below $15 \mu\text{m}^1$. Moreover, $G_{Ic,i}$ values from the insert are usually lower than those from precracks. On the other hand, it can be argued that crack initiation from the film does not occur under self-similar conditions. In fact, the distribution of G_I along the width of a DCB specimen with a straight crack is not uniform, due to anticlastic curvature of the specimen arms^{6,7}. Figure 3 shows a width-wise distribution of G_I in C/epoxy specimens obtained from a 3D FE analysis⁶. Naturally, under steady-state propagation, a curved delamination front develops, so that $G_I = G_{Ic}$. This would favour the use of mode I precracks.

Currently, however, the standards recommend that $G_{Ic,i}$ are measured from both film and mode I precrack, to be generated in a first precracking test^{1,2}.

Another question concerning initiation is the definition of the exact instant when it occurs. Three criteria are proposed in ISO 15024² (figure 4): the non-linearity (NL); the 5% offset or maximum load point (5/M) and the visually (VIS) determined. The NL criterion defines crack initiation at the point where the load-displacement curve deviates from linearity. Besides giving the most conservative values, the NL criterion seems to correlate with Acoustic Emission detections¹. It has been shown, however, that locating the NL point is somewhat dependent on the plot scale. The 5/M criterion stipulates that a line corresponding to a compliance 5 % larger than the initial one is intersected with the actual load-displacement curve (figure 4). This intersection point is taken as initiation, unless it occurs at a larger displacement than the maximum load point. In the latter case, initiation is precisely the point of maximum load. Although less ambiguous, the 5/M criterion tends to give higher $G_{Ic,i}$ values than the other criteria, even for materials with relatively mild R -curves (figure 5). Moreover, the 5% value is obviously arbitrary. Finally, the VIS criterion is operator dependent, but this limitation could be compensated by the increasing use of video recording of the tests. Nevertheless, it is highly unlikely that VIS detection from the film will be accurate, as crack growth at the edges tends to occur later than in the middle of the specimen.

2.2. Mode II

In contrast with mode I, there is much more controversy about the measurement and meaningfulness of the mode II fracture toughness⁸⁻¹⁰. It has been argued that the microcracks observed in the tests are actually oriented at approximately 45° from the fibre direction, thus showing that crack propagation is locally mode I dominated¹¹. Nevertheless, most of the present design approaches are based on Macromechanics and many structures are subjected to bending loads, which naturally give rise to significant mode II. Moreover, it was found that the compression after impact strength of composite plates was proportional to the mode II critical strain energy release rate, G_{IIc} , of unidirectional specimens¹².

Various test configurations have been proposed to measure G_{IIc} ^{1,9}(figure 6): end-notched flexure (ENF); end-loaded split (ELS) and 4-point end-notched flexure (4ENF).

Owing to its simplicity, the ENF specimen has been the most used, in spite of the inherently unstable crack propagation. Stabilisation is possible in servo-controlled testing machines, which, however, are not always available and increase the complexity of the test setup^{1,9}. The main advantage of the ELS specimen is precisely the stability of crack

propagation if $a/L > 0.55$ (figure 6), but the specimen is more prone to large displacements and to variable clamping conditions⁸. There is still little experience with the 4ENF test, which seems to combine the simplicity of ENF with the stability of ELS. Comparisons between the various test methods have not yet been able to indicate “the best method”^{9,10}.

The effect of friction has also been raised as a possible problem in mode II tests. However, numerical analyses have showed small friction effects in ENF and 4ENF specimens^{1,10}.

On the other hand, the problems concerning crack initiation mentioned above are even more relevant in mode II testing. Figure 7 shows the results obtained from ENF tests on glass/epoxy specimens⁸ using Corrected Beam Theory¹³

$$G_{IIc} = \frac{9a^2 P^2}{16b^2 E h^3} \left[1 + 0.2 \frac{E}{G} \left(\frac{h}{a} \right)^2 \right] \frac{F_2}{N_2}, \quad (2)$$

where E and G are the specimen flexural and shear moduli, respectively, and F_2 and N_2 are correction factors for large displacements¹³. Precracking seems to be of great relevance, since initiation G_{IIc} from mode I and mode II precracks were significantly lower than those from the film (figure 7). As to defining crack initiation, in this case, the NL criterion lead to unacceptably low G_{IIc} values because it was associated with the onset of large displacements. The 5/M criterion did not seem to be significantly affected, but it still gave somewhat higher values than visual detection. However, the contact between the cracked arms of the specimens makes visual detection more difficult than in mode I, especially in carbon fibre composites.

When performing ENF tests from a mode II precrack, the exact precrack length a must be determined. Glass fibre composites are usually translucent, thereby enabling visual determination of the precrack position. This is generally not the case of carbon fibre composites. Therefore, ESIS recommends the compliance calibration¹³

$$C = C_o + ma^3 \quad (3)$$

giving

$$G_{IIc} = \frac{3ma^2 P^2}{2b}, \quad (4)$$

although its accuracy may be affected by a low m coefficient.

3. MULTIDIRECTIONAL LAMINATES

3.1. Mode I

In spite of the remaining questions discussed above, it is clear that mode I and mode II testing of UDs have reached a reasonable degree of maturity. In practice, however, the vast majority of applications involves multidirectional specimens (MDs), and delaminations always occur between layers of different orientations. It is thus essential to obtain toughness values of MDs for the applicability of Fracture Mechanics based design approaches.

Several studies have already been presented on DCB testing of MDs^{6,14-22}. The first difficulty with MDs is the selection of appropriate stacking sequences. In fact, significant errors in G_{Ic} measurements may be caused by the elastic membrane-bending and bending-bending couplings of MDs^{7,23}. Particular attention should be given to avoiding excessive anticlastic curvature of the specimen arms, which results in highly curved thumbnail shaped delamination fronts. The magnitude of anticlastic effects is proportional to the parameter $D_c = D_{12}^2/(D_{11}D_{22})$, where D_{ij} represent the Classical Lamination Theory (CLT) bending stiffness coefficients of each specimen arm^{7,23}. It has been suggested that DCB specimens should have $D_c < 0.25$ ^{7,23}. Bending-twisting and membrane-bending elastic couplings should also be minimised. The former can be characterised by the $B_t = |D_{16}/D_{11}|$ parameter and could cause markedly unsymmetrical delamination fronts. The latter may introduce relevant contributions of thermal residual stresses to the measured G_{Ic} ^{23,24}. Membrane-bending couplings are absent when both cracked and uncracked parts of the specimens are symmetric about their own mid-planes. However, this is not possible when the delamination is placed between interfaces of different orientations, which is precisely the case of greater practical interest.

There is also a theoretical problem with cracking between layers of different orientations, because the stress field is oscillatory in the vicinity of such cracks²⁵⁻²⁸. Consequently, although the total strain energy release rate G is well defined, its individual components G_I , G_{II} and G_{III} cannot be determined using their classical definition, since the crack extension integrals do not tend to a limit as the crack extension increment Δa tends to 0²⁵⁻²⁸. This mode partitioning ambiguity can be solved by considering “finite extension strain energy release rates”, where Δa should be set equal to a characteristic damage zone length, l_c ^{27,28}. Based on stress field analysis and on interlaminar strength properties, it has been shown that l_c is of the order of the layer thickness^{27,28}.

From the practical viewpoint, the major problem with MDs is clearly the high tendency for intraply cracking and crack jumping between neighbouring interfaces. The complex

damage morphology leads to pronounced R -curves, with final apparent G_{Ic} values 3 to 4 times higher than those of $[0^\circ]_n$ specimens. Figure 8 shows R -curves obtained from DCB tests on carbon/epoxy $[0^\circ]_{24}$ and cross-ply $[(0^\circ/90^\circ)_6// (0^\circ/90^\circ)_6]$ specimens, where $//$ denotes the starter crack position⁶. Crack propagation in the latter involved periodical cracking of the 90° mid-layer and interlaminar crack growth in the neighbour $0^\circ/90^\circ$ interfaces, as schematically depicted in figure 9. However, recorded data points always corresponded to local interlaminar propagation. In those conditions, an FE analysis indicated that the measured G_{Ic} were valid⁶. Although no significant fibre bridging was observed, some non-linearity in the load-displacement curve might have contributed to the much higher G_{Ic} .

In order to avoid crack jumping problems, Robinson and Song¹⁸ proposed the edge pre-delaminated (EPD) DCB specimen (figure 10). While crack jumping was avoided, the monitoring of crack position became difficult, due to the contact between the pre-delaminated edges²⁹. Moreover, recent numerical analyses showed that the EDP-DCB specimen is inadequate to measure initiation G_{Ic} ³⁰. Another important drawback is that intralaminar damage is not always avoided¹⁹.

Using thick (over 6 mm, 48 layers) and narrow (between 4 and 10 mm) specimens, Chai observed pure interlaminar propagation in MD CFRP specimens¹⁵. Measured toughnesses were practically identical for specimens with delaminations on $0^\circ/0^\circ$, $45^\circ/-45^\circ$, $0^\circ/45^\circ$ and $0^\circ/90^\circ$ interfaces. It is important to mention that the delamination was not placed at the specimen mid-thickness, a feature that could generate significant mode-mixity effects. Nevertheless, numerical analyses³⁰ showed that accurate G_{Ic} can be obtained with those specimens, which thus require more experimental studies.

3.2. Mode II

As in mode I, intralaminar damage affected many of the mode II toughness results for MDs presented thus far³¹⁻³⁷. Again, with thick and narrow ENF specimens, Chai was able to obtain pure interlaminar propagation in C/epoxy and C/PEEK specimens with $30^\circ/-30^\circ$ delaminating interfaces³¹. The specimens with $30^\circ/-30^\circ$ interfaces presented significantly higher G_{IIc} , especially for a brittle matrix C/epoxy composite. Studies involving GRPs and specimens with θ - θ delaminating interfaces indicate a θ -increasing G_{IIc} ^{31,33,35,37}. This trend is easily interpreted in terms of larger plasticity zones ahead of the crack tip. However, observed non-linearity for GRPs specimens with $\theta \geq 30^\circ$ casts doubts about the validity of the measured G_{IIc} values^{31,37}.

On the other hand, results from ENF tests on flat filament wound glass/polyester specimens revealed an intermediate G_{IIc} decrease from $\theta \approx 0.8^\circ$ (hoop winding) to $\theta = 5^\circ$ (figure 11). This somewhat unexpected variation could be due to the particular nature of filament wound specimens, combined with a strong effect of the thickness of the resin rich interlaminar layer, as hoop wound specimens have a higher degree of compactation. In fact, Chai³¹ showed that G_{IIc} of adhesive joints was highly sensitive to the adhesive layer thickness. It is very likely that this effect is present in laminated composites, because of fibre nesting in UD. Therefore, it seems essential to study the mode II interlaminar fracture of specimens with θ/θ interfaces at low θ .

Tao and Sun have investigated several types of MD carbon/epoxy ENF specimens³⁴. They observed that, as a result of intralaminar cracking, the delamination always jumped to a $0^\circ/\theta$ Interface. They subsequently tested specimens with starter delaminations on such interfaces, and succeeded in avoiding intralaminar cracking by positioning the specimens so that the θ -oriented layer would be under compression. In those circumstances, G_{IIc} decreased for $\theta = 0^\circ$ to 90° , thus reinforcing the interest in studying mode II fracture of composites.

4. CONCLUSIONS, ONGOING AND FUTURE RESEARCH

The present review of the state-of-the-art in mode I and mode II interlaminar fracture testing of composites shows the need to pursue research on three major topics:

- crack initiation criteria;
- mode II specimen configuration;
- testing of multidirectional specimens (MDs).

The latter is highly relevant, as structural applications usually involve MD laminates, with delaminations developing between layers of different orientations. Furthermore, some results indicate that the common tests on unidirectional $[0^\circ]_n$ specimens (UDs) may not give the lowest G_{IIc} values. MD stacking sequences must be carefully chosen to minimise the effects of curved delamination fronts, mode-mixity and residual stresses on G_c measurements. Current efforts³⁰ have been devoted to “design” MDs using 3D FE analyses. The intralaminar damage and crack jumping phenomena common to MDs are now the main obstacle. A current experimental programme is being carried out with thick MDs, since it was reported that they were free from those difficulties^{15,31}.

The often observed R -curves make the exact definition of crack initiation particularly important. In fact, the R -curve is usually associated to fibre bridging and crack jumping

phenomena that are specimen geometry dependent. Furthermore, such phenomena tend to occur in the initial stages of crack propagation, and especially in MDs. At this level, experimental work will be complemented with progressive damage based numerical simulations. Initiation criteria will be evaluated by comparing predicted G_c values with those inputted into the damage model³⁰.

As to the choice of the “best” mode II specimen, the 4ENF specimen seems to be quite promising. The testing rig is simple, and crack propagation is stable. However, the practical difficulty in following crack propagation and the greater interest in crack initiation may not provide significant advantages over the ENF specimen. Moreover, the suitability for MDs is an important factor still to be evaluated. MDs are generally less rigid and, according to some studies, could also be tougher than UD. One can expect more difficulties with the ELS specimen e.g. large displacements and intralaminar damage. Considering the relevance of MDs and the available results, the present experimental work is being carried out with the ENF specimen, though studies on the ELS and 4ENF geometries are continuing elsewhere.

ACKNOWLEDGEMENTS

Most of the work herein presented was performed in the scope of Round Robins organised by the Technical Committee 4 (TC4) of the European Structural Integrity Society (ESIS). The authors wish to thank the other members of TC4 for their cooperation and for providing the specimens.

Several projects in Portugal (JNICT and FCT) or in the European Union also contributed to the understanding of interlaminar fracture. In particular, A. B. de Morais thanks the Portuguese Foundation for Science and Technology (research project POCTI/EME/38731/2001, FEDER European Union fund) for supporting the work currently being performed on the subject.

REFERENCES

1. Davies P (1998), Blackman BRK, Brunner AJ. Standard test methods for delamination resistance of composite materials: current status. *Appl. Compos. Mater.*, **5**, 345-364.
2. ISO 15024:2001. Fibre-reinforced plastic composites - Determination of mode I interlaminar fracture toughness, G_{Ic} , for unidirectionally reinforced materials.
3. Friedrich K, Carlsson LA, Gillespie JW, Karger-Kossis J (1991). Fracture of thermoplastic composite materials. In *Thermoplastic composite materials*. Edited by L.A. Carlsson. Elsevier Science.
4. Hashemi S, Kinloch AJ, Williams JG (1990). Mechanics and mechanisms of delamination in a Polyether Sulfone-fibre composite. *Compos. Sci. Technol.*, **37**, 429-462.

5. Davies P et al. (1992). Round-Robin interlaminar fracture testing of carbon-fibre-reinforced epoxy and PEEK composites. *Compos. Sci. Technol.*, **43**, 129-136.
6. Morais AB, Moura MF, Marques AT, Castro PT (2002). Mode I interlaminar fracture of carbon/epoxy cross-ply composites. *Compos. Sci. Technol.*, **62**, 679-686.
7. Davidson BD (1990). An analytical investigation of delamination front curvature in double cantilever beam specimens. *J. Compos. Mater.*, **24**, 1124-1137.
8. Davies P, Ducept F, Brunner AJ, Blackman BRK, Morais AB (1996). Development of a standard mode II shear fracture test procedure. In *Proceedings of ECCM-7, London*, 9-15.
9. Davies P et al (1999). Comparison of test configurations for determination of mode II interlaminar fracture toughness: results from international collaborative test programme. *Plastics, Rubber and Composites*, **28**, 432-437.
10. Schuecker C, Davidson BD (2000). Evaluation of the accuracy of the four-point bend end-notched flexure test for mode II delamination toughness determination. *Compos. Sci. Technol.*, **60**, 2137-2146.
11. O'Brien TK (1998). Composite interlaminar shear fracture toughness, G_{IIc} : shear measurement or sheer myth? *ASTM STP 1330*, 3-18.
12. Evans RE, Masters JE (1987). A new generation of epoxy composites for primary structural applications: materials and mechanics. *ASTM STP 937*, 413-421.
13. *Fracture Mechanics Testing Methods for Polymers, Adhesives and Composites* (2001). ESIS Publication 28. Edited by D. R. Moore, A. Pavan, J. G. Williams. Elsevier Science Ltd.
14. Nicholls DJ, Gallagher PJ (1983). Determination of G_{Ic} in angle ply composites using a cantilever beam test method. *J. Reinf. Plast. Compos.*, **2**, 2-17.
15. Chai H (1984). The characterization of mode I delamination failure in non-woven multidirectional laminates. *Composites*, **15**, 277-290.
16. Schapery RA, Goetz DP, Jordan WM (1986). Delamination analysis of composites with distributed damage using a J integral. *Proc. Int. Symp. on Compos. Mater. Struct., Beijing*, 543-549.
17. Laksimi A, Benzeggagh ML, Jing G, Hecini M, Roelandt JM (1991). Mode I interlaminar fracture of symmetrical cross-ply laminates. *Compos. Sci. Technol.*, **41**, 147-164.
18. Robinson P, Song DQ (1992). A modified DCB specimen for mode I testing of multi-directional laminates. *J. Compos. Mater.*, **26**, 1554-1577.
19. Choi NS, Kinloch AJ, Williams JG (1999). Delamination fracture of multidirectional carbon-fibre/epoxy composites under mode I, mode II and mixed-mode I/II loading. *J. Compos. Mater.*, **33**, 73-100.
20. Ozdil F, Carlsson LA (1999). Beam analysis of angle-ply laminate DCB specimens. *Compos. Sci. Technol.*, **59**, 305-315.
21. Benyahia AA, Benzeggagh ML, Gong XL (2000). Initiation and bifurcation mechanisms of cracks in multi-directional laminates. *Compos. Sci. Technol.*, **60**, 597-604.
22. Rhee KY, Koh SK, Lee JH (2000). Mode I fracture resistance characteristics of graphite/epoxy laminated composites. *Polym. Compos.*, **21**, 155-164.
23. Davidson BD, Krüger R, König M (1996). Effect of stacking sequence on energy release rate distributions in multidirectional DCB and ENF specimens. *Eng. Fract. Mech.*, **55**, 557-569.

24. Nairn JA (2000). Energy release rate analysis for adhesive and laminate double cantilever beam specimens emphasizing the effect of residual stresses. *Int. J. Adhesion and Adhesives*, **20**, 59-70.
25. Raju IS, Crews JH, Aminpour MA (1988). Convergence of strain energy release rate components for edge-delaminated composite laminates. *Eng. Fract. Mech.*, **30**, 383-396.
26. Qian W, Sun CT (1997). Calculation of stress intensity factors for interlaminar cracks in composite laminates. *Compos. Sci. Technol.*, **57**, 637-650.
27. Narayan SH, Beuth JL (1998). Designation of mode mix in orthotropic composite delamination problems. *Int. J. Fract.*, **90**, 383-400.
28. Chow WT, Atluri SN (1997). Stress intensity factors as fracture parameters for delamination crack growth in composite laminates. *Composites*, **28B**, 375-384.
29. Robinson P, Javidrad F, Hitchings D (1995). Finite element modelling of delamination growth in the DCB and edge delaminated DCB specimens. *Compos. Struct.*, **32**, 275-285.
30. Morais AB, Moura MF, Gonçalves JPM, Camanho PP (2003). Analysis of crack propagation in Double Cantilever Beam tests of multidirectional laminates. *Mech. Mater.*, **35**, 641-652.
31. Chai H (1990). Interlaminar shear fracture of laminated composites. *Int. J. Fract.*, **43**, 117-131.
32. Polaha JJ, Davidson BD, Hudson RC, Pieracci A (1996). Effects of mode ratio, ply orientation and precracking on the delamination toughness of a laminated composite. *J. Reinf. Plast. Compos.*, **15**, 141-173.
33. Ozdil F, Carlsson LA, Davies P (1998). Beam analysis of angle-ply laminate end-notched flexure specimens. *Compos. Sci. Technol.*, **58**, 1929-1938.
34. Tao JX, Sun CT (1998). Influence of ply orientation on delamination in composite laminates. *J. Compos. Mater.*, **32**, 1933-1947.
35. Choi NS, Kinloch AJ, Williams JG (1999). Delamination fracture of multidirectional carbon-fiber/epoxy composites under mode I, mode II and mixed-mode I/II loading. *J. Compos. Mater.*, **33**, 73-100.
36. Hwang JH, Kwon O, Lee CS, Hwang W (2000). Interlaminar fracture and low velocity impact of carbon/epoxy composite materials. *Mech. Compos. Mater.*, **36**, 195-214.
37. Morais AB, Silva JF, Marques AT, Castro PT (2002). Mode II interlaminar fracture of filament wound angle-ply specimens. *Appl. Compos. Mater.*, **9**, 117-129.

FIGURES

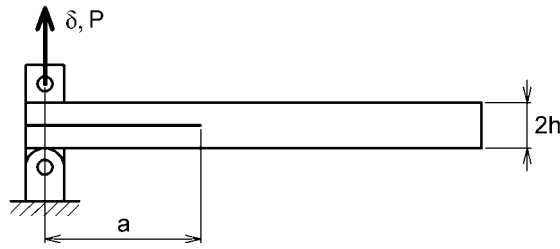


Figure 1. Scheme of the DCB test.

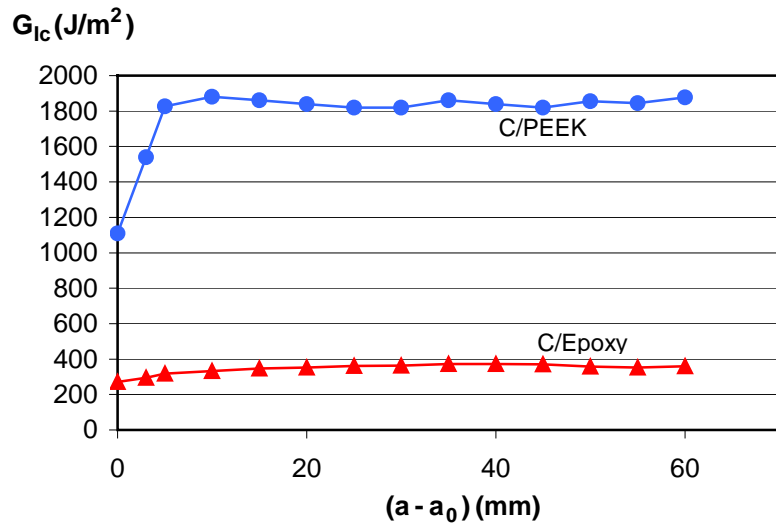


Figure 2. Typical R -curves obtained in DCB tests of C/PEEK⁵ and C/epoxy⁶ UD specimens.

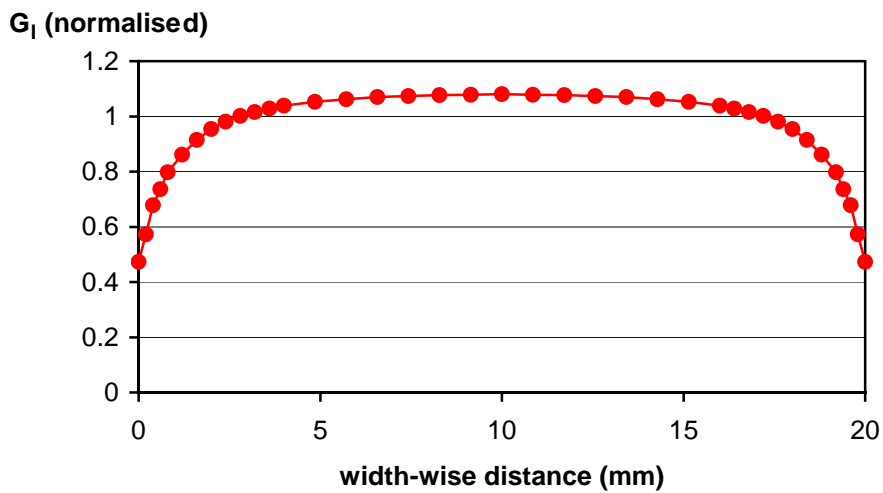


Figure 3. Distribution of G_I along the width of C/epoxy UD specimens⁶. G_I values were normalised by the width-wise average.

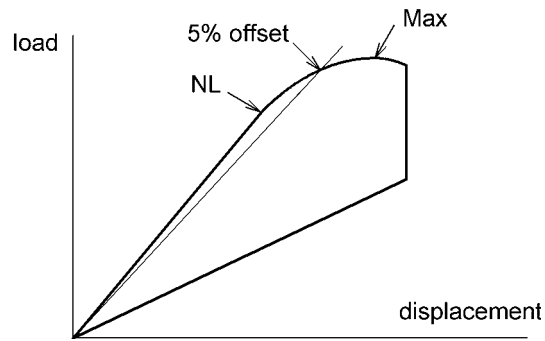


Figure 4. Alternative crack initiation criteria^{1,2}.

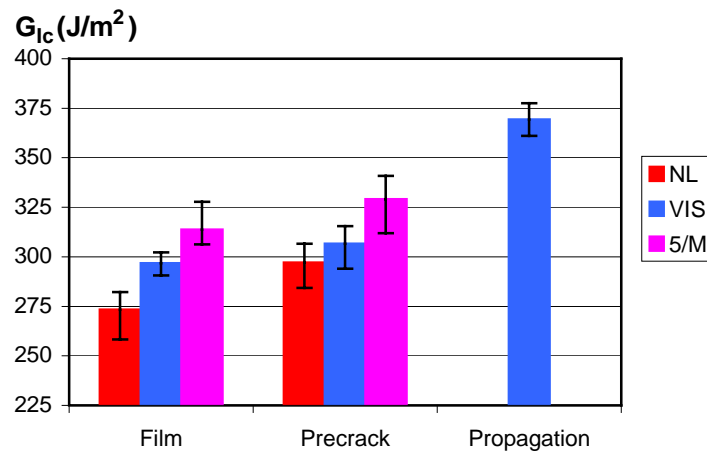


Figure 5. Results of DCB tests on C/epoxy UD specimens according to the various initiation criteria⁶. Propagation values are also included.

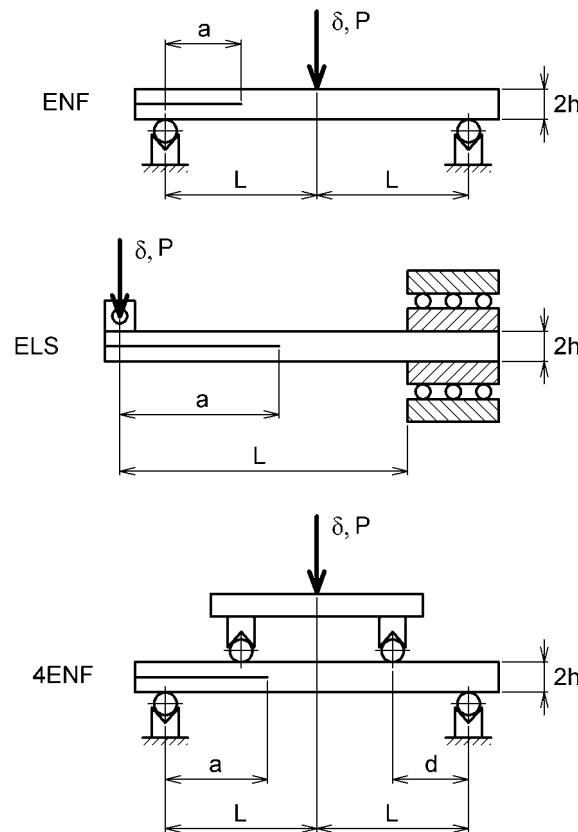


Figure 6. Schematic representation of the proposed mode II specimens.

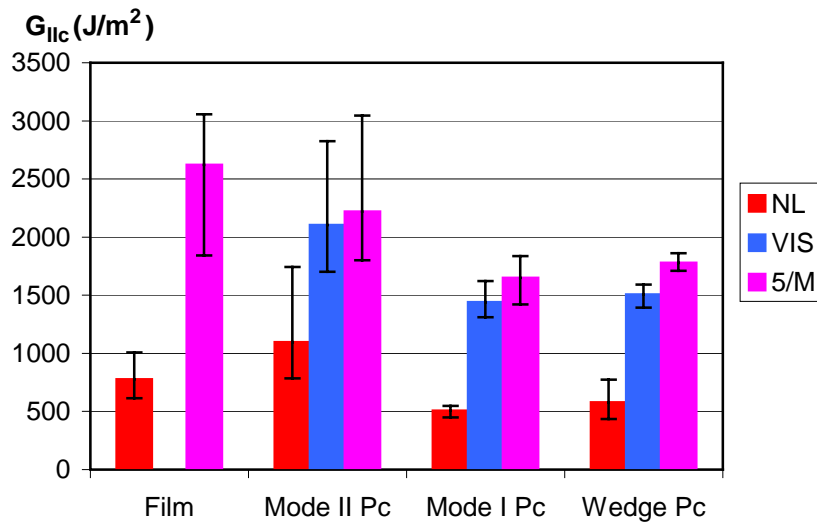


Figure 7. Results of ENF tests on glass/epoxy UD specimens: influence of the starter defect (film, mode I, mode II and wedge precracks) and of initiation criteria⁸.

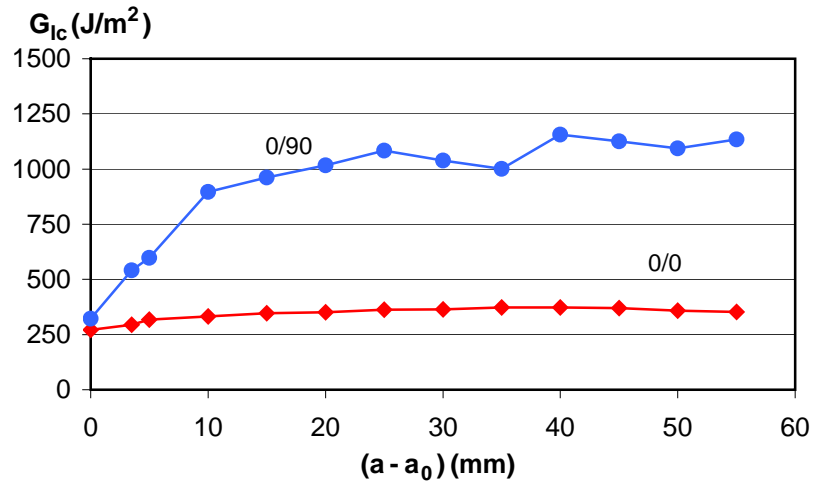


Figure 8. Typical R -curves of C/epoxy $[(0^\circ/90^\circ)_6 // (0^\circ/90^\circ)_6]$ and $[0^\circ_{12} // 0^\circ_{12}]$ specimens⁶.

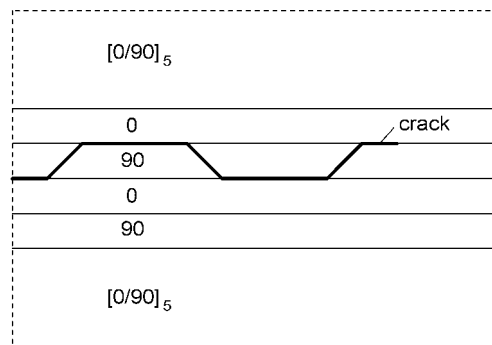


Figure 9. Scheme of crack propagation in $[(0^\circ/90^\circ)_6 // (0^\circ/90^\circ)_6]$ specimens⁶.

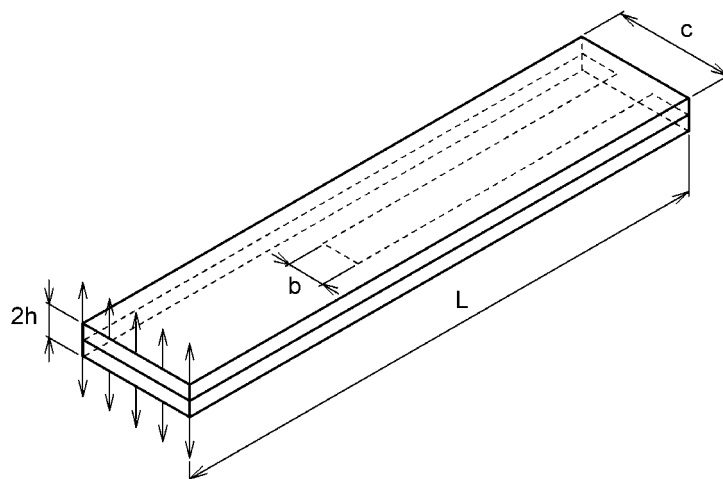


Figure 10. Schematic representation of the edge pre-delaminated (EPD) DCB specimen¹⁸.

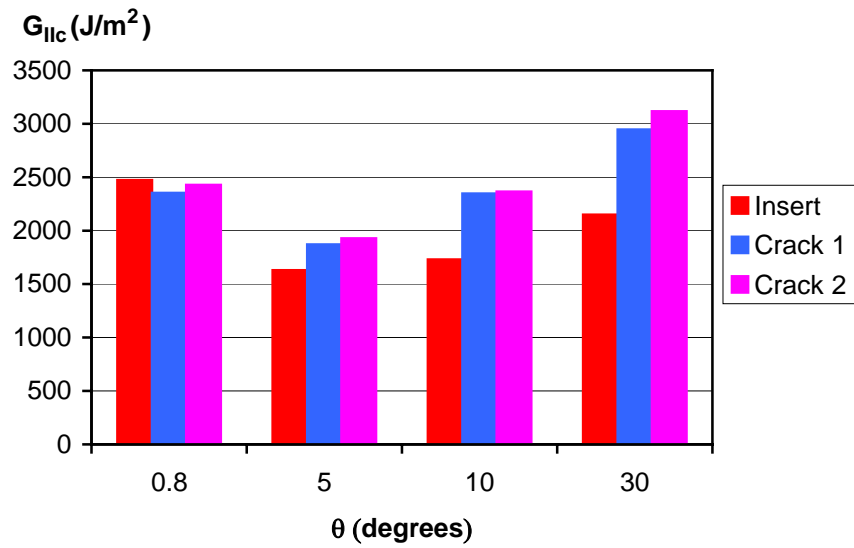


Figure 11. Results of ENF tests on glass/polyester flat filament wound specimens³⁷.